BJPS

Brazilian Journal of Pharmaceutical Sciences

http://dx.doi.org/10.1590/s2175-97902020000118738

Article

Blockage of TGF-β1-induced epithelial-to-mesenchymal transition by oxymatrine prevents renal interstitial fibrosis

Li Li[1*], Dongyuan He[2], Qin Cai[1], Dong-ying Wang[1]

[1]Department of Nephrology, The Second Affiliated Hospital of Nanjing University of Chinese Medicine, Jiangsu Second Chinese Medicine Hospital, Nanjing, China; [2]Department of Nephrology, Zhejiang Hospital, Hangzhou, China

Most chronic kidney disease inevitably progress to renal fibrosis. Tubular epithelial-to-mesenchymal transition (EMT) is recognized to play major roles in renal fibrosis. Oxymatrine (OM) is a major alkaloid component found in a Chinese herb Sophora roots and has many effects. The aim is to investigate the effect of OM on renal tubular EMT and elucidate its mechanism. Mice underwent unilateral ureteral obstruction (UUO) followed by intraperitoneal injection of OM (120 mg/kg) or control vehicle. Human kidney proximal tubular cell line (HK-2) was used and EMT was induced with 5 ng/mL of transforming growth factor-β1 (TGF-β1). *In vivo*, renal tubulointerstitial fibrosis was induced and E-cadherin was down-regulated, while the expressions of fibronectin (FN), α-smooth muscle actin (α-SMA), TGF-β1 and its type I receptor (TGF-βRI) were up-regulated in UUO mice. In contrast, OM significantly ameliorated renal fibrotic lesions and attenuated the expressions of FN, α-SMA, TGF-β1 and TGF-βRI, but increased E-cadherin in the obstructed kidneys. *In vitro*, OM abolished TGF-β1-mediated E-cadherin suppression and FN, α-SMA and TGF-βRI induction in HK-2 cells in a dose-dependent manner. These observations strongly suggest that the renal protective effects of OM could be mediated by prevention of EMT and manifested as suppression of TGF-β1 and TGF-βRI expressions.

Keywords: Oxymatrine. Renal tubulointerstitial fibrosis. Epithelial-to-mesenchymal transition. Transforming growth factor-β1

INTRODUCTION

Renal Tubulointerstitial fibrosis (TIF) is the final common pathway in chronic kidney disease (CKD) leading to functional deterioration and eventual loss of renal function (Farris, Colvin, 2012). TIF is characterized by tubular atrophy and increased interstitial matrix deposition. Although many different cell types and cytokines are involved, α-smooth muscle actin (α-SMA)-positive myofibroblasts are the principal effect cells in fibrotic kidney and transforming growth factor-β1 (TGF-β1) plays the central role to promote the myofibroblastic activation (Hills, Squires, 2011). A common notion was that activated myofibroblasts arise primarily from resident fibroblasts, recent evidence has demonstrated activated myofibroblasts can also arise from tubular epithelial cells (TECs) via epithelial-to-mesenchymal transition (EMT) (Xavier *et al.*, 2015; Hills *et al.*, 2012). Recent studies using genetic models provide strong evidence for a pivotal role of EMT in renal fibrogenesis (Cruz-Solbes, Youker, 2017). Tubular EMT

***Correspondence:** L. Li. Department of Nephrology. The Second Affiliated Hospital of Nanjing University of Chinese Medicine, Jiangsu Second Chinese Medicine Hospital. 23 south lake Road, Nanjing City, Jiangsu Province, PR China. Phone: +86 25 8329 1250, +86 182 0518 7587; Fax: +86 25

is a process in which renal TECs lose their epithelial phenotype and acquire new characteristic features of mesenchymal cells. These TECs lose the epithelial cell marker E-cadherin and acquired mesenchymal features such as α-SMA and vimentin, and produce interstitial matrix components such as fibronectin (FN) and collagen (Xavier *et al*., 2015; Cruz-Solbes, Youker, 2017; Lan, 2003). TGF-β1 alone can initiates and completes the entire EMT course (Xavier *et al*., 2015; Cruz-Solbes, Youker, 2017; Iwano, 2010).

Oxymatrine (OM) is a major alkaloid component found in a Chinese herb Sophora roots. OM has a tetracyclic quinolizine structure. Its molecular formula is C15H24N2O2 Figure 1. It has been shown that OM has anti-inflammatory and antiviral effects (Song *et al*., 2006). In recent years, OM has been used in the treatment of chronic liver disease and has a significant effect on the inhibition of liver fibrosis (Jiang *et al*., 2005; Shi, Li, 2005). However, the role of OM in renal fibrosis is less understood. In the present study, we explored the therapeutic efficacy of OM on renal TIF and investigated its potential mechanism.

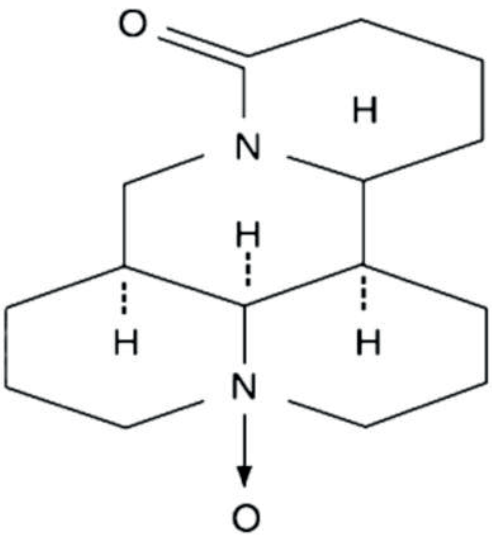

FIGURE 1 - The chemical structure of oxymatrine

MATERIAL AND METHODS

Material

OM Injection (H20057480) with a purity of more than 98% was purchased from Zheng-Da-Tian-Qing Pharmaceutical Co. Ltd., China. Recombinant human TGF-β1 (240-B) and TGF-β1 ELISA Development kit (DY1679) were purchased from R&D Systems (Minneapolis, MN, USA). Monoclonal antibodies against FN (sc-71113), TGF-β1 type I receptor (TGF-βRI) (sc-398) and α-tubulin (sc-58667) were purchased from Santa Cruz Biotechnology (Santa Cruz, CA, USA). Anti-α-SMA (A2547) was purchased from Sigma (St Louis, MO, USA). Primary antibody against E-cadherin (4065) was from Cell Signaling Technology (Beverly, MA, USA). Dulbecco's Modified Eagle's Medium/F12 was from Invitrogen (San Diego, CA, USA) and fetal calf serum (FCS) obtained from Gibco-BRL (Gaithersburg, MD, USA).

CD1 mice weighing 18 to 20 g, were obtained from the Shanghai Experimental Animal Center. They were housed in the Experimental Animal Center at Nanjing University of Chinese Medicine with free access to food and water. Animals were treated humanely in accordance with NMAC guidelines and approved protocols of the Nanjing University of Chinese Medicine Animal Use and Care Committee. Thirty-six mice were randomly divided into 3 groups: sham group, unilateral ureteral obstruction (UUO) group and UUO with OM (UUO-OM) therapy group. Each group has 12 mice. UUO was performed according to established procedure (Yang, Liu, 2001). Briefly, under general anesthesia, complete ureteral obstruction was performed by double ligation of the left ureter by 4-0 silk, through midline abdominal incision. Mice of sham group had their ureters exposed but not ligated. OM was diluted with normal saline. After operation mice of OM treatment group were given OM (120 mg/kg per day) by intraperitoneal injection, sham and UUO mice were given same volume of vehicle. Six mice of each group were killed at day 3 (UUO-3d-OM group) and day 7 (UUO-7d-OM group) after UUO operation respectively. One part of the kidneys was fixed in 10% phosphate-buffered formalin, followed by paraffin embedding for pathological studies. The remaining kidneys were snap-frozen in liquid nitrogen and stored at -80 °C for ELISA and protein studies.

Methods

Histological and pathological staining

Kidney sections with 4 μm thickness from paraffin-embedded tissues were made by using a routine procedure. Sections were stained with

hematoxylin/eosin (HE) for general histology. Another set of sections was stained using the Masson's trichrome staining method for identifying interstitial collagen by blue color. A morphological analysis was made for semi-quantitatively determining the extent of tubulointerstitial injury. Briefly, 5 visions (upper left, lower left, upper right, lower right and middle) were observed under low magnification per section, each of 8 parameters of tubulointerstitial injury (TEC degeneration, tubular dilatation, tubular atrophy, red cell cast, protein cast, interstitial edema, interstitial fibrosis and interstitial infiltration of inflammatory cells) were assigned by scores from 0 to 3 according to the severity (0= no abnormality, 1= mild, 2= moderate, 3= severe), and these scores of each mouse were summed to define the overall tubulointerstitial score (TIS). The pathologist was blinded to study design.

Western blot analysis

Kidney samples were homogenized in radioimmune precipitation assay lysis buffer (1% Nonidet P-40, 0.1% sodium dodecyl sulfate (SDS), 100 μg/mL phenylmethylsulfonyl fluoride, 0.5% sodium deoxycholate, 1 mmol/L sodium orthovanadate, 2 μg/mL aprotinin, 2 μg/mL antipain, and 2 μg/mL leupeptinin phosphate-buffered saline) on ice by using a homogenizer. The supernatants were gathered after centrifugation at 13000 g at 4 °C for 20 min. Protein concentration was decided by using a bicinchoninic acid protein assay kit, and whole tissue lysates were mixed with an equal amount 2×SDS loading buffer (125 mmol/L Tris–HCl, 4% SDS, 20% glycerol, 100 mmol/L dithiothreitol, and 0.2% bromphenol blue). Samples were heated at 100 °C for 5 min before loading and then separated on 10% SDS-polyacrylamide gels. The proteins were electrotransferred to a nitrocellulose membrane in transfer buffer containing 48 mmol/L Tris-HCl, 39 mmol/L glycine, 0.037% SDS and 20% methanol at 4 °C for 1 H. Nonspecific binding to the membrane was blocked for 1 H at room temperature with 5% nonfat milk in TBS buffer (20 mmol/L Tris–HCl, 150 mmol/L NaCl, and 0.1% Tween 20). The membranes were then incubated for 16 H at 4 °C with various primary antibodies in blocking buffer containing 5% milk at the dilutions specified by the manufacturers, followed by incubation with horseradish peroxidase-conjugated secondary antibody for 1 H in 5% nonfat milk dissolved in Tris-buffered saline. Membranes were then washed with Tris-buffered saline, and the signals were visualized using the enhanced chemiluminescence system. Quantification was performed by measurement of the intensity of the bands with the use of NIH Image analysis software.

Enzyme-linked immunosorbent assay

To detect renal TGF-β1 concentrations, kidneys from mice were homogenized in the extraction buffer containing 20 mM Tris-HCl, pH 7.5, 2 M NaCl, 0.1% Tween 80, 1 mM ethylenediamine tetraacetate and 1 mM phenylmethylsulfonyl fluoride, and the supernatant was recovered after centrifugation at 19000 g for 20 min at 4 °C. Renal tissue TGF-β1 level were measured by using the commercial TGF-β1 ELISA development kit (DY1679) in accordance with the protocol specified by the manufacturer.

Cell culture

The HK-2 cells were obtained from the Cell Resource Center of the Shanghai Institutes for Biological Sciences. Cells were culture at density of 0.2×10^5 in DMEM/F12 supplemented with 10% fetal bovine serum. For TGF-β1 treatment 24 H later, serum-free medium was added to cells, prior 16 H incubation. TGF-β1 and OM were added at a final concentration of 5 ng/mL and 360 mg/L or as indicated for various periods of time. The cells were incubated for 48 H before harvesting for western blot or immunofluorescence staining.

MTT assay

The effect of OM on cell viability was assessed by MTT (3-[4,5-dimethyl-2-thiazolyl]-2, 5-diphenyl-2-tetrazoliumbromide) assay. 1×10^4 cells per well were seeded onto 96-well plates and cultured for 24 H, and then treated with OM with different concentrations for another 24 H. After that, MTT solution was added to final concentration 0.5 mg/mL. The cells were incubated for 4 H and the medium was transferred into blue formazan crystals that dissolved in 150 μL dimethylulfoxide (DMSO). The absorbance was measured at 490 nm using a microplate reader and the arithmetic mean OD of 8 wells for each group was calculated. The experiment was technical repeated at least 3 times.

Indirect immunofluorescence staining

Indirect immunofluorescence staining was made by using an established procedure (Yang, Liu, 2001). Briefly, HK-2 cells, cultured on coverslips, were washed with cold phosphate-buffered saline (PBS) twice, and fixed with cold methanol:acetone (1:1) for 10 min at -20 °C. Following extensive washing with PBS containing 0.5% bovine serum albumin (BSA) for three times, the cells were blocked with 0.1% Triton X-100 and 2% BSA in PBS buffer for 40 min at room temperature, and then incubated with the specific primary antibodies in PBS containing 2% BSA overnight at 4 °C. After extensive wash, cells were incubated for 1 H with FITC-Labeled secondary antibodies provided by the Immunol Fluorence Staining Kit (Zhongshan Goldenbridge Biotechnology CO., LTD.) at a dilution of 1:50. As a negative control, the primary antibody was replaced with non-immune IgG, and no staining occurred. Cells were double stained with DAPI (4',6-diamidino-2-phenylindole, HCl) to visualize the nuclei. Slides were mounted with Vectashield anti-fade mounting media and viewed with a Nikon Eclipse 80i Epi-fluorescence microscope equipped with a digital camera. In each experimental setting, immunofluorescence images were captured with identical light exposure times.

Statistical analysis

All data examined were expressed as mean ± SEM. Statistical analysis was performed using SigmaStat software. Comparison among groups was made with one-way ANOVA, and this was followed by the Student-Newman-Keuls test. Multiple comparisons tests were applied only when a significant difference was determined on the ANOVA ($P < 0.05$). $P < 0.05$ was considered statistically significant.

RESULTS AND DISCUSSION

Results

OM reduces renal fibrosis in obstructive nephropathy

To assess the potential effect of OM on renal fibrosis, mice were given OM (120 mg/kg) by intraperitoneal injection or vehicle after UUO. Figure 2 shows representative micrographs of the HE and Masson's trichrome staining of renal tissue sections at 3 day or 7 day after UUO. In mice treated with control vehicle, extensive periductal and interstitial collagen deposition was evident, as shown by positive Masson's staining. Fibrosis could be detected in the renal interstitial area at 3 day and was more severe at 7 day. However, delivery of OM largely inhibited renal interstitial collagen accumulation after UUO. To quantitatively evaluate the therapeutic efficacy of OM on renal interstitial injury induced by UUO, we determined the tubulointerstitial score from 8 parameters as mentioned previously. As shown in Figure 2M, the tubulointerstitial score was progressively increased at 3 day and 7 day after UUO. However, OM substantially reduced the tubulointerstitial score in the renal tissue sections at different time points Figure 2.

OM treatment attenuated increased expressions of FN and α-SMA and decreased E-cadherin in UUO kidneys

Western blot analysis revealed that the expressions of FN and α-SMA were very weak in the renal tubule and interstium of normal kidneys, whereas they were prominent in model rats especially when the disease progressed. On the other hand, E-cadherin decreased and was continuously downregulated in UUO-7d group (Figure 3). OM treatment attenuated the increased expressions of FN and α-SMA, especially in UUO-3d group. Moreover, E-cadherin expression was maintained and was continuously effective in UUO-7d group Figure 3.

OM suppresses the expression of TGF-β1 and its Type I receptor in the obstructed kidneys

As presented in Figure 4A, UUO induced a dramatic increase in renal TGF-β1 expression. The steady-state levels of TGF-β1 in the kidney at 7 day after UUO were increased about more than 8-fold, compared to the sham. However, administration with OM markedly suppressed renal TGF-β1 abundance. The expression of TGF-βRI in the kidney was also examined at different time points after UUO by western blot. As shown in Figure 4B and C, OM significantly altered renal TGF-βRI expression at 3 day and 7 day after UUO.

OM treatment attenuated TGF-β1-induced EMT in HK-2 cells

For cell viability assay 1×10^4 cells per well were seeded onto 96-well plates with 200 μL of DMEM. The

cells were cultured for 24 H before treatment with OM at different concentrations and cell survival was assessed by MTT. As shown in Figure 5A, the relative viability of cells was slightly increased by OM in a range of 60- 360 mg/L, while above the concentration of 360 mg/L, OM showed a mild inhibition on the viability of HK-2 cells although there was no statistically significant difference. It suggested the appropriate concentration of OM was safe to prevent the EMT of HK-2 cells.

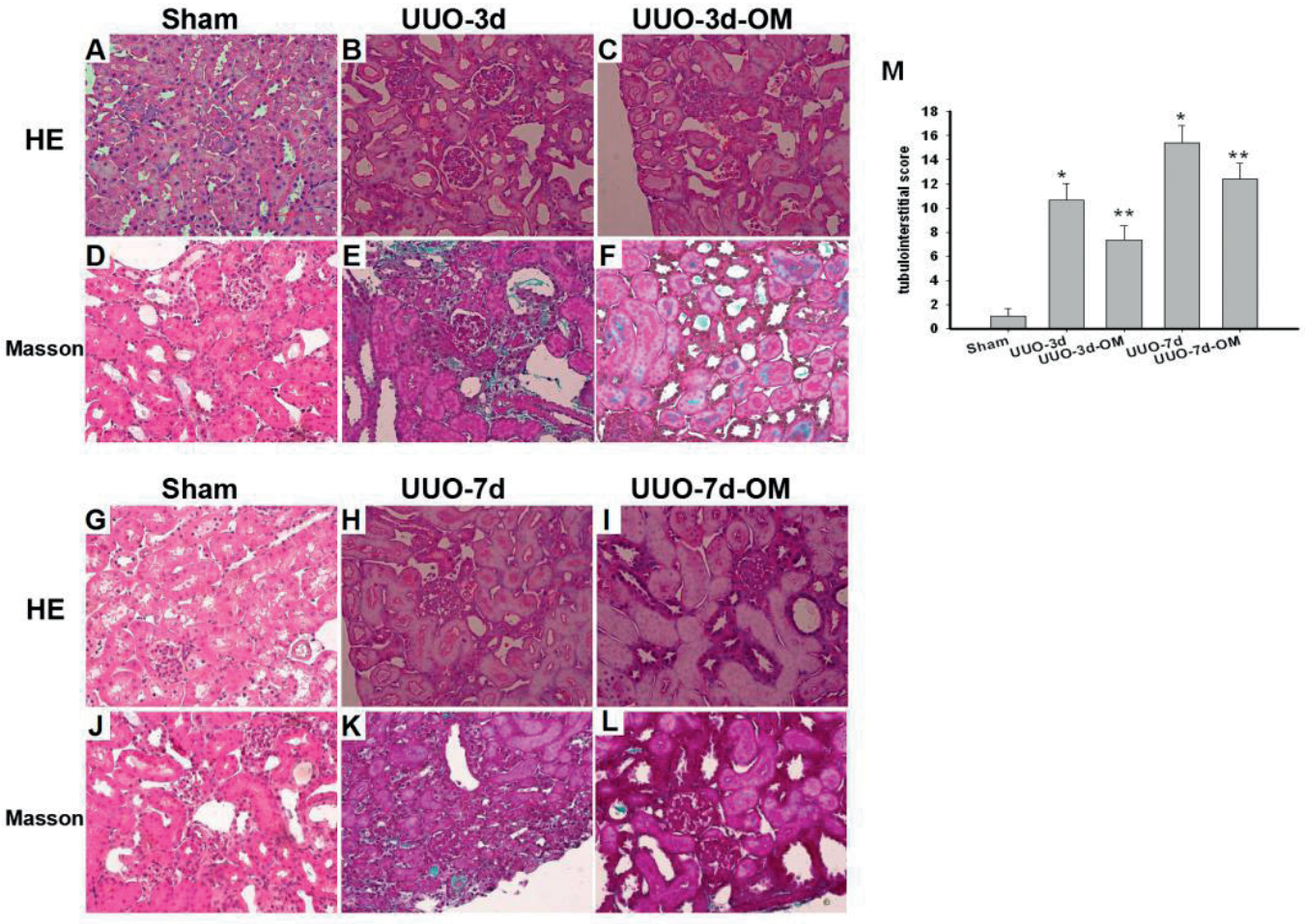

FIGURE 2 - HE/Masson staining (A- L) and tubulointerstitial score (M) of Sham, UUO-3d or UUO-7d with or without OM treatment

OM treatment can significantly ameliorate the degree of obstructive nephropathy and reduce the tubulointerstitial score. The pictures are representative of at least 3 independent technical experiments performed in duplicate. Original magnification×400. *: P<0.01 vs. sham group, **: P<0.05 vs. each UUO group, respectively (n = 6).

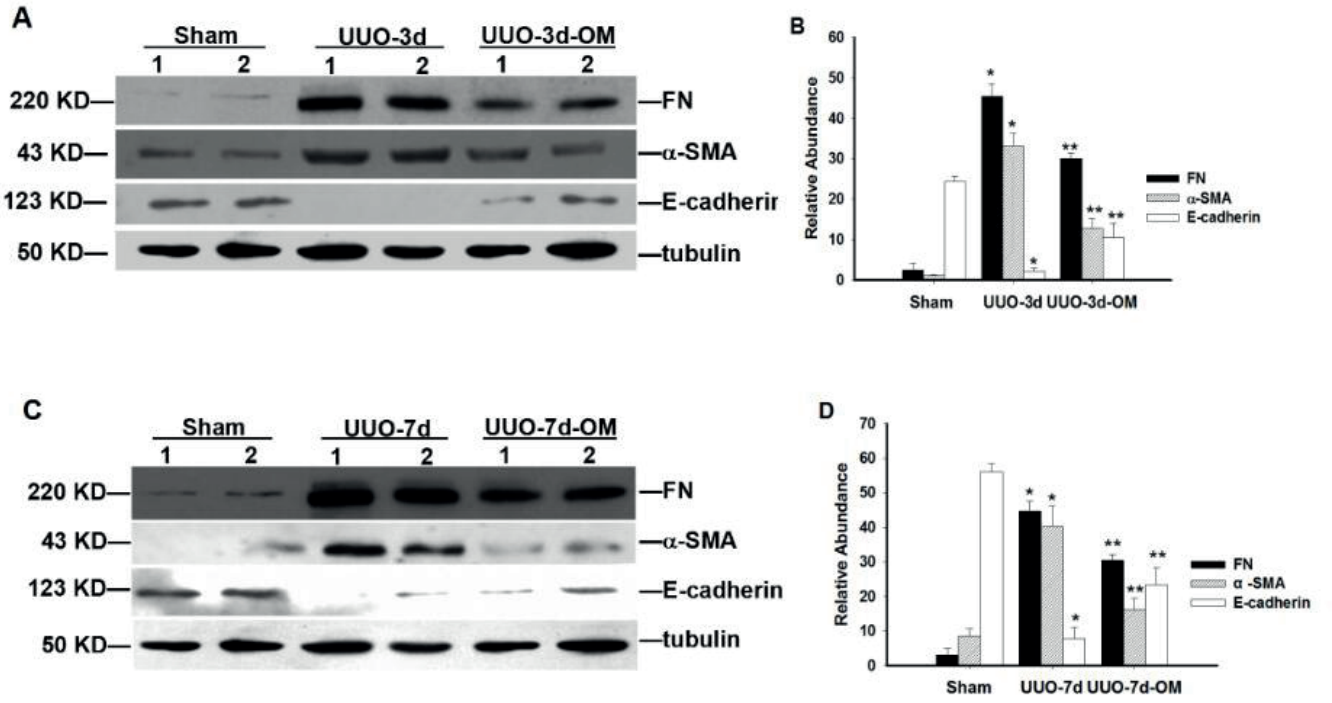

FIGURE 3 - OM inhibits FN, α-SMA and preserves epithelial E-cadherin expressions in UUO groups
Western blot analyses for FN, α-SMA and E-cadherin expressions in renal tissues. Increased labeling of FN and α-SMA were observed in UUO-3d and UUO-7d groups, while those were noted to be decreased by OM treatment. E-cadherin labeling intensity was decreased in model mice, whereas it was also recovered in the OM treatment group (A and C). Graphic presentation of the relative expressions of FN, α-SMA and E-cadherin (B and D). The graph summarizes densitometric analysis of 3 independent technical experiments. The values are represented as the density of FN, α-SMA or E-cadherin vs tubulin control. *: $P<0.05$ vs. sham group, **: $P<0.05$ vs. UUO-3d group.

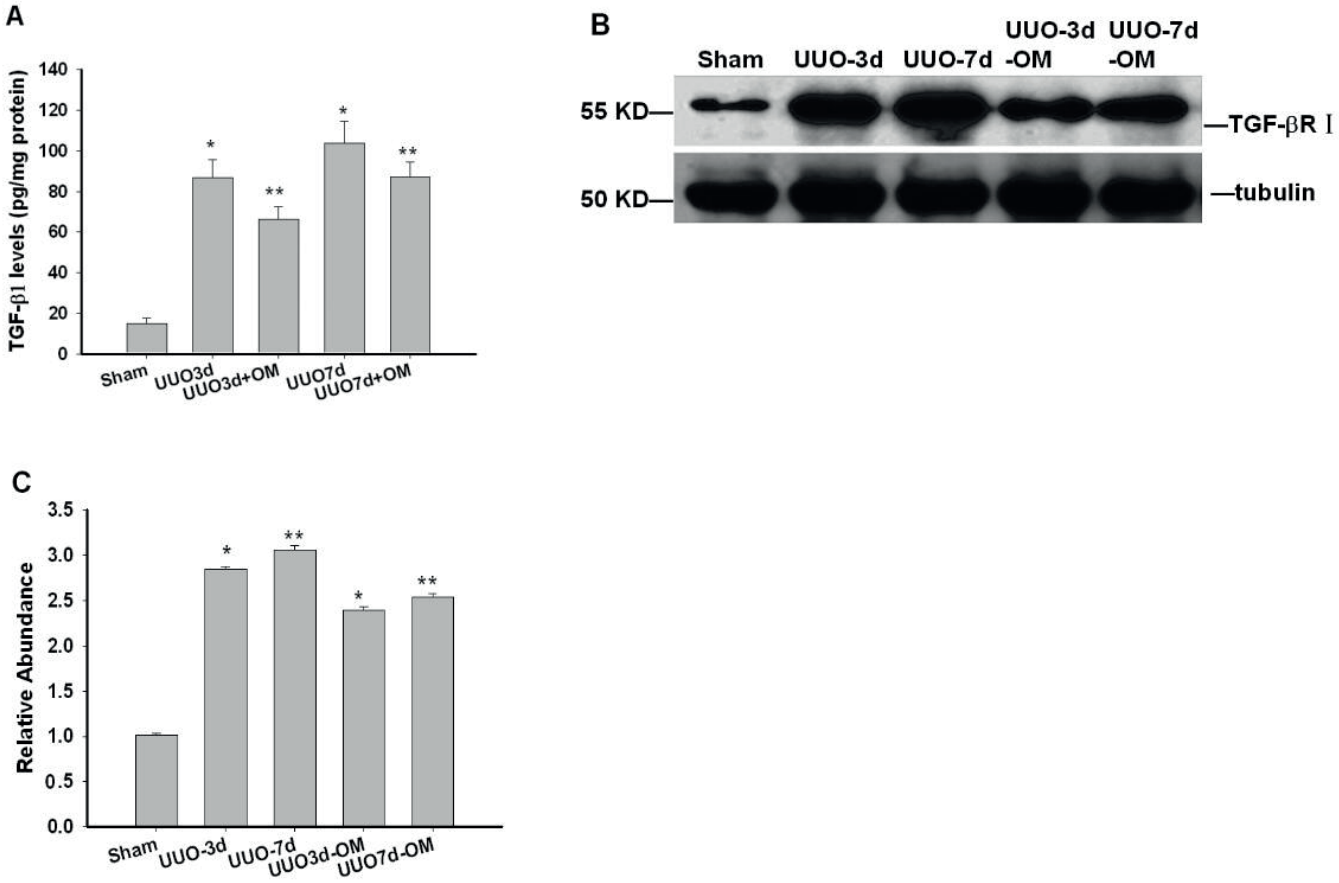

FIGURE 4 - TGF-β1 protein levels were determined by ELISA in the kidneys at 3d or 7 d after UUO with or without OM treatment and sham group

The protein levels of TGF-β1 type I receptor at 3 d or 7 d after UUO with or without OM. OM reduced the TGF-β1 and its type I receptor (TGF-βRI) levels of renal tissues in UUO mice. The values are represented as the density of TGF-βRI vs tubulin control. The graph summarizes densitometric analysis of 3 independent technical experiments. *: P<0.05 vs. sham group, **: P<0.05 vs. UUO-3d and UUO-7d group respectively.

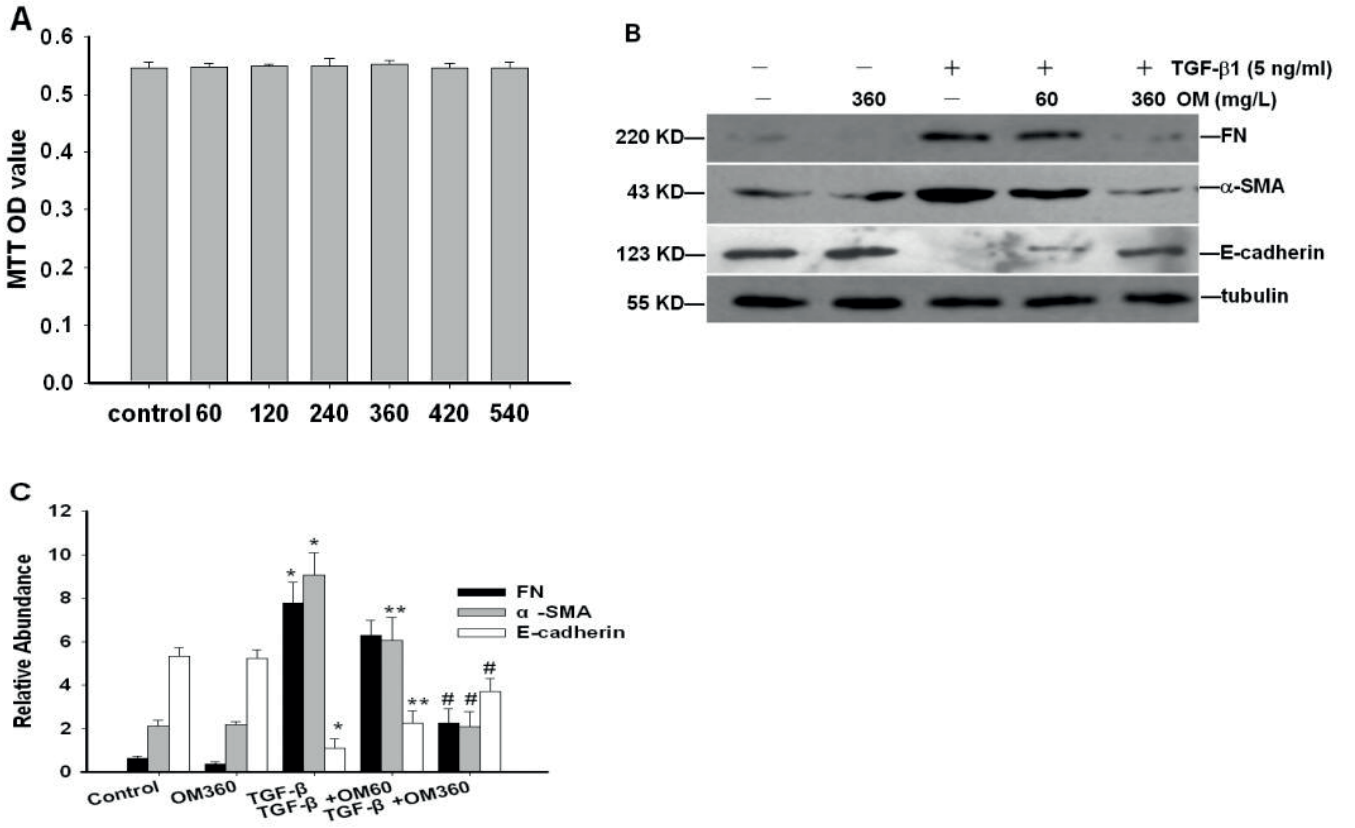

FIGURE 5 - The dose response effect of OM on proliferation of HK-2 cells
At the concentration of 60- 360 mg/L, OM increased cell viability in a dose-dependent manner, while above 360 mg/L this effect is not obvious although there was no statistically significant difference (A). OM blocks TGF-β1-mediated EMT *in vitro*. HK-2 cells were treated without (control) or with 5 ng/ml TGF-β1 in the presence or absence of various concentrations of OM as indicated for 48 H (B and C). Western blot showed that OM restored E-cadherin expression that was inhibited by TGF-β1 in a dose-dependent manner, whereas it suppressed TGF-β1-mediated induction of FN and α-SMA. Whole-cell lysates were immunoblotted with antibodies against FN, α-SMA, E-cadherin and tubulin, respectively. Densitometric analysis of three independent technical experiments (B and C). The data were normalized by the density of tubulin control. *: P<0.05 vs. control group, **: P<0.05 vs. TGF-β1 group, #: P<0.05 vs. TGF-β1 group, respectively.

After treatment with TGF-β1, HK-2 cells began to lose epithelial adhesion receptor E-cadherin and began to markedly produce the components of interstitial matrix (such as FN) and gained α-SMA expression. However, treatment with OM inhibited the TGF-β1-mediated EMT in a dose dependent manner. Western blot exhibited that OM restored E-cadherin expression, whereas it inhibited TGF-β1-mediated induction of FN and α-SMA (Figure 5B and 5C). These results were further confirmed by indirect immuneoflurescence showing HK-2 cells at basal conditions expressed trivial amounts of FN (Figure 6A, D and G) and α-SMA (Figure 6J, M and P), abundant E-cadherin (Figure 6S, V and Y). However, after activation by TGF-β1, the HK-2 cells became activated, principal matrix producing cells that expressed a striking amounts of interstitial FN (Figure 6B, E and H) and α-SMA (Figure 6K, N and Q), rapidly decreased E-cadherin (Figure 6T, W and Z). Simultaneous incubation with OM (360 mg/L) strongly blocked the TGF-β1-induced expressions of FN (Figure 6C, F and I) and α-SMA (Figure 6L, O and R), restored E-cadherin (Figure 6U, X and &).

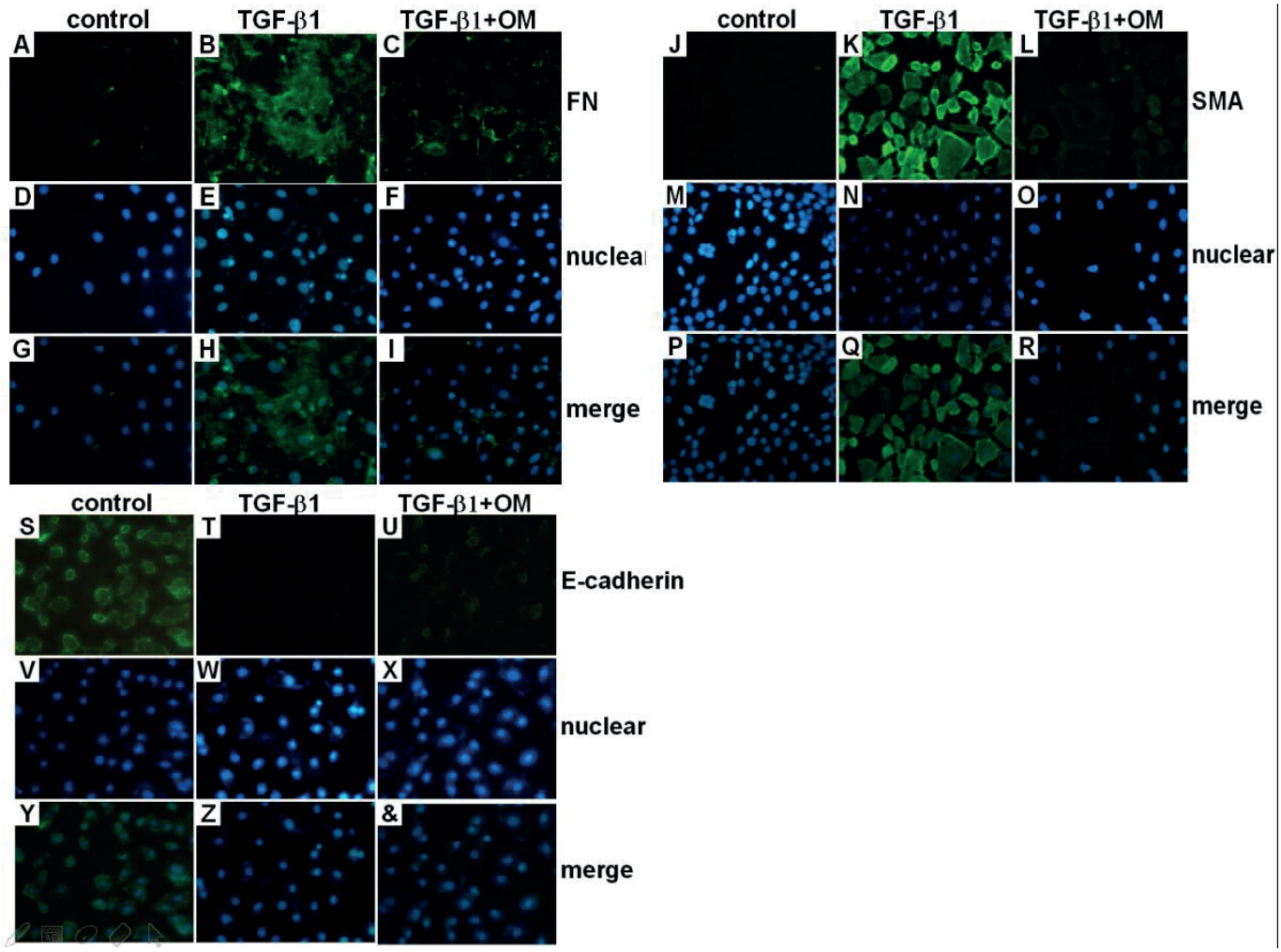

FIGURE 6 - Immunofluorescence staining demonstrated that OM blocks TGF-β1-mediated EMT in HK-2 cells
Immunofluorescent microscopy of FN (A through I), α-SMA (J through R) and E-cadherin (S through &) in HK-2 cells after various treatments. HK-2 cells were treated without (A, J, S) or with TGF-β1 at 5 ng/mL (B, K, T), or TGF-β1 plus 360 mg/L of OM (C, L, U) for 48 h. Basline FN (A, G), α-SMA (J, P) and E-cadherin (S, Y) in HK-2 cells. FN (B, H) and α-SMA (K, Q) upregulated and E-cadherin (T, Z) downergulated after TGF-β1 treatment. The increased immunolabeling intensity of FN, α-SMA and the decreased intensity of E-cadherin in response to TGF-β1 stimuli were reversed by OM treatment (C and I, L and R, U and &). Nuclear staining for DAPI is shown (D- F, M- O and V- X) and merged results are also demonstrated (G- I, P- R and Y- &). The graph summarizes densitometric analysis of 3 independent technical experiments. Magnification A- &: ×400.
OM treatment attenuated the expression of TGF-βRI in HK-2 cells activated by TGF-β1

We incubated the HK-2 cells with 5 ng/mL TGF-β1 for 48 H to induce EMT. As shown in Figure 7, the protein expression of TGF-βRI in HK-2 cells was significantly increased after incubation with TGF-β1 (5 ng/mL), while it was inhibited by OM in a dose-dependent manner.

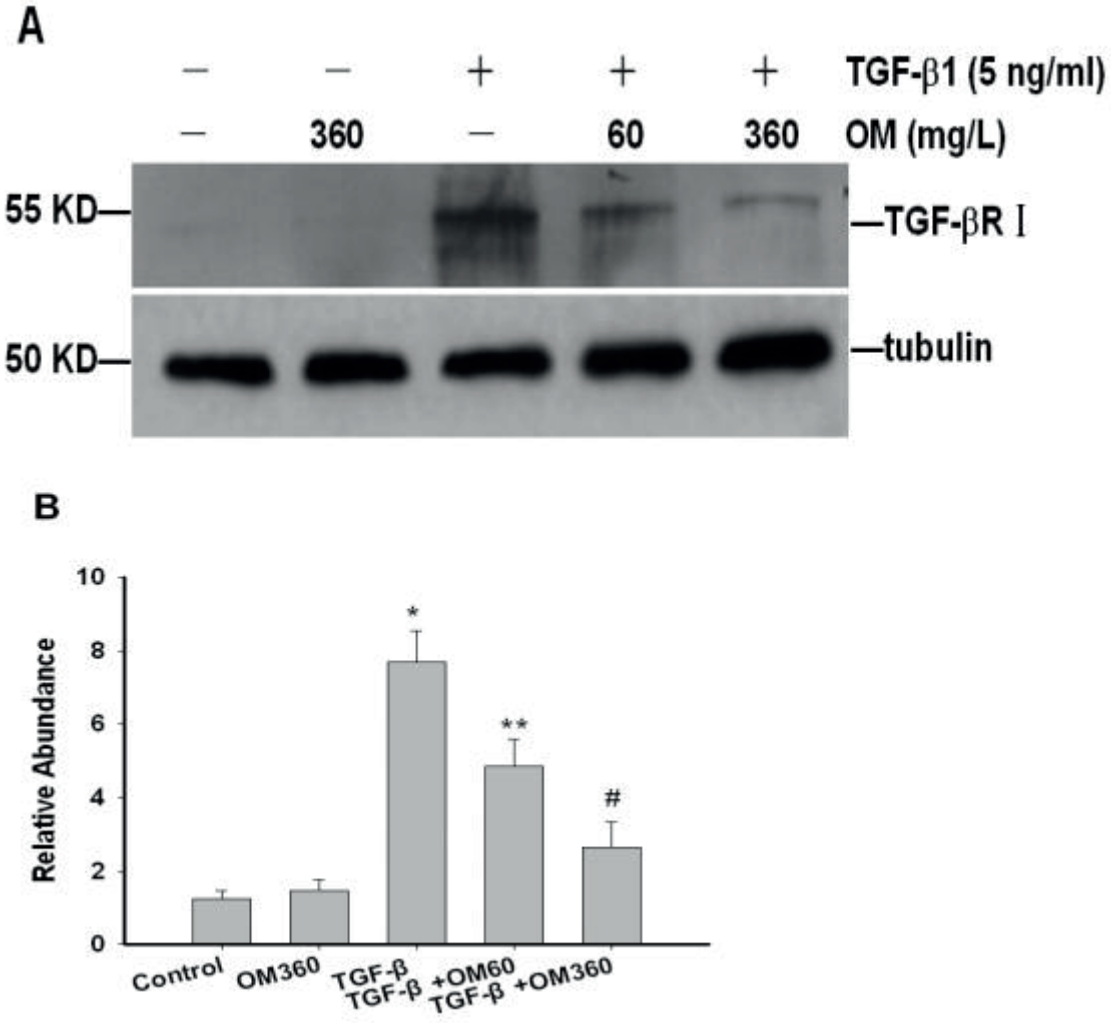

FIGURE 7 - OM treatment attenuated the expression of TGF-βRI in HK-2 cells activated by TGF-β1
HK-2 cells were incubated with TGF-β1 (5 ng/ml) or/and various concentrations of OM for 48 H. The protein expression of TGF-βRI in HK-2 cells was significantly increased after incubation with TGF-β1 (5 ng/ml), while it was inhibited by OM in a dose-dependent manner (A). Graphical presentation of the relative abundance of TGF-βRI after normalization with α-tubulin control in different groups. The graph summarizes densitometric analysis of 3 independent technical experiments. *: P<0.05 vs. control group, **: P<0.05 vs. TGF-β1 group, #: P<0.01 vs. TGF-β1 group.

DISCUSSION

Renal TIF is often regarded as a final, common pathway of many forms of CKD (Farris, Colvin, 2012). Clinical studies suggest that in patients with CKD, the decline in renal function often correlates more closely with the extent of TIF lesions than with those of glomerular injury (Yanagita, 2012; Nogueira, Pires, Oliveira, 2017). So renal interstitial fibrosis is considered the hallmark of progressive renal disease. Fibroblasts are considered the primary matrix-producing cells in the kidney and hence they are clinically relevant as principal mediators of renal fibrosis associated with progressive renal failure (Li *et al.*, 2011). Fibroblasts are regarded as mesenchymal cells that display a spindleshaped morphology, under pathological conditions, they can rapidly proliferate, produce interstitial collagens, and contribute to the progression of tissue fibrosis. Various stimuli have been found to induce fibroblast activation. Fibroblasts become activated to myofibroblasts by stimulation

with cytokines including TGF-β1, fibroblast growth factor-2 and others. In general, fibroblasts respond to stimuli associated with tissue injury by acquiring an activated phenotype myofibroblasts. Interstitial myofibroblasts are much more heterogeneous than expected and they might come from interstitial resident fibroblasts, circulating fibrocytes, EMT-derived fibroblasts, and other cells of mesenchymal origin, such as pericytes (Barnes, Glass, 2011). Among them, the most plausible explanation for the replenishment of myofibroblasts during fibrogenesis is EMT. Iwano *et al*. (2002) showed that during renal fibrogenesis, interstitial myofibroblasts are derived in small numbers from bone marrow, pericytes and in large numbers from local EMT (up to 36% of additional ECM-producing myofibroblasts derived EMT). As a consequence of EMT, tubular cells become the matrix-producing myofibroblasts, resulting in overproduction of the interstitial matrix components (Carew, Wang, Kantharidis, 2012). Since specific therapies of preventing the progression of CKD are still lacking, seeking drug candidates or herbal compounds that can effectively prevent EMT would represent one of the main strategies in the treatment of renal TIF.

OM is an alkaloid extracted from the traditional Chinese herb Sophora flavescens. Several studies have shown that OM produces a variety of pharmacological actions (Wang, Han, Zhu, 2015; Xiao, 2012). It was originally used for the treatment of chronic viral hepatitis. Later, it was found that OM inhibits the proliferation of fibroblasts (Wu *et al*., 2008; Deng *et al*., 2009). Shi and Li (2005) found OM has an interference effect on hepatic fibrosis, probably by reducing the expression level of tissue inhibitor of metalloproteinase-1 in rat liver tissues.

To our knowledge, there are no reports on the effects of OM treatment could be applied to inhibit the process toward renal fibrosis. For studying the antifibrotic effect of OM, we used the UUO mice to induce renal fibrosis. As UUO model mimics, in an accelerated manner, the different stages of obstructive nephropathy leading to tubulointerstitial fibrosis, including cellular infiltration, EMT, (myo)fibroblast accumulation, increased ECM deposition (Bascands, Schanstra, 2005). These different features of the pathology appear rapidly, all within around one week after the induction of the pathology and are highly reproducible from one experiment to another. Based on the above reasons, the UUO model was prepared by CD1 mice to study the treatment of renal fibrosis by OM. Our results demonstrated that OM markedly suppresses ECM expression and attenuates renal fibrosis in UUO mice (see in Figure 2 and 3). The inhibitory role of OM in tubular EMT is corroborated further by *in vitro* studies, in which OM is able to block directly the TGF-β1-mediated EMT in HK-2 cells. In this study, indirect immuneoflurescence and western blot both reveled exposure of HK-2 cells to TGF-β1 for 48 H induced a complete conversion of the epithelial cells to myofibroblasts as evidenced by acquisition of FN and α-SMA, loss of E-cadherin (Figure 6B and 7). However, treatment with OM exhibited a remarkable inhibitory effect on TGF-β1-induced EMT in cultured cells (Figure 5B and 6). Hence, blockade of EMT by OM could be an imperative mechanism that accounts for its renoprotective action in the pathogenesis of TIF. These observations also highlight the effectiveness and efficacy of OM as a potential therapeutic agent for inhibiting EMT and interstitial fibrogenesis in the diseased kidneys.

Next we examine the effect of OM on the TGF-β1 and its type I receptor expression. Expressions of TGF-β1 and TGF-βRI increased significantly after UUO operation in a time dependent manner. However, administration with OM markedly suppressed renal TGF-β1 and TGF-βRI proteins in UUO mice (Figure 4). As shown in Figure 7, the results demonstrated that the protein expression of TGF-βRI in HK-2 cells was initiated expression through TGF-β1 stimuli, while it was significantly decreased by OM treatment in a dose-dependent manner. So the inhibitory role of OM in EMT is probably through reducing the TGF-β1 and its receptor levels.

Although UUO models do not reliably reflect the clinical setting and other kidney fibrosis animal studies (such as uninephroctomized and subtotally nephroctomized models) and ongoing clinical trials are required, this study suggests that OM was able to retard TGF-β1 expression in the obstructed kidneys and the progression of renal fibrosis in mice. Moreover, OM attenuated the TGF-β1-induced EMT in HK-2 cells, and this could be mediated by attenuation of the TGF-β1-induced upregulation of TGF-βRI. In this regard, the present study not only suggest that OM could be applied to inhibit the process toward renal fibrosis, at least partly by attenuating EMT, but also sets a foundation for the rational utilization of OM in combating renal fibrosis.

REFERENCES

Barnes JL, Glass WF. Renal interstitial fibrosis: a critical evaluation of the origin of myofibroblasts. Contrib Nephrol. 2011;169:73-93.

Bascands JL, Schanstra JP. Obstructive nephropathy: insights from genetically engineered animals. Kidney Int. 2005;68(3):925-37.

Carew RM, Wang B, Kantharidis P. The role of EMT in renal fibrosis. Cell Tissue Res. 2012;347(1):103-16.

Cruz-Solbes AS, Youker K. Epithelial to Mesenchymal Transition (EMT) and Endothelial to Mesenchymal Transition (EndMT): role and implications in kidney fibrosis. Results Probl Cell Differ. 2017;60:345-72.

Deng ZY, Li J, Jin Y, Chen XL, Lü XW. Effect of oxymatrine on the p38 mitogen-activated protein kinases signalling pathway in rats with CCl4 induced hepatic fibrosis. Chin Med J. 2009;122(12):1449-54.

Farris AB, Colvin RB. Renal interstitial fibrosis: mechanisms and evaluation. Curr Opin Nephrol Hypertens. 2012;21(3):289-300.

Hills CE, Siamantouras E, Smith SW, Cockwell P, Liu KK, Squires PE. TGFβ modulates cell-to-cell communication in early epithelial-to-mesenchymal transition. Diabetologia. 2012;55(3):812-24.

Hills CE, Squires PE. The role of TGF-β and epithelial-to mesenchymal transition in diabetic nephropathy. Cytokine Growth Factor Rev. 2011;22(3):131-39.

Iwano M. EMT and TGF-beta in renal fibrosis. Front Biosci (Schol Ed). 2010;2:229-38.

Iwano M, Plieth D, Danoff TM, Xue C, Okada H, Neilson EG. Evidence that fibroblasts derive from epithelium during tissue fibrosis. J Clin Invest. 2002;110(3):341-50.

Jiang H, Meng F, Li J, Sun X. Anti-apoptosis effects of oxymatrine protect the liver from warm ischemia reperfusion injury in rats. World J Surg. 2005;29(11):1397-401.

Lan HY. Tubular epithelial-myofibroblast transdifferentiation mechanisms in proximal tubule cells. Curr Opin Nephrol Hypertens. 2003;12(1):25-9.

Li L, He D, Yang JW, Wang X. Cordycepin inhibits renal interstitial myofibroblast activation probably by inducing hepatocyte growth factor expression. J Pharmacol Sci. 2011;117(4):286-94.

Nogueira A, Pires MJ, Oliveira PA. Pathophysiological mechanisms of renal fibrosis: a review of animal models and therapeutic strategies. *In Vivo*. 2017;31(1):1-22.

Shi GF, Li Q. Effects of oxymatrine on experimental hepatic fibrosis and its mechanism *in vivo*. World J Gastroenterol. 2005;11(2):268-71.

Song G, Luo Q, Qin J, Wang L, Shi Y, Sun C. Effects of oxymatrine on proliferation and apoptosis in human hepatoma cells. Colloids Surf B Biointerfaces. 2006;48(1):1-5.

Wang B, Han Q, Zhu Y. Oxymatrine inhibited cell proliferation by inducing apoptosis in human lung cancer A549 cells. Biomed Mater Eng. 2015;26(Suppl 1):S165-72.

Wu XL, Zeng WZ, Jiang MD, Qin JP, Xu H. Effect of oxymatrine on the TGFbeta-Smad signaling pathway in rats with CCl4-induced hepatic fibrosis. World J Gastroenterol. 2008;14(13):2100-5.

Xavier S, Vasko R, Matsumoto K, Zullo JA, Chen R, Maizel J, et al. Curtailing endothelial TGF-β signaling is sufficient to reduce endothelial-mesenchymal transition and fibrosis in CKD. J Am Soc Nephrol. 2015;26(4):817-29.

Xiao L, Ge Y, Sun LX, Xu X, Xie P, Zhan M, et al. Cordycepin inhibits albumin-induced epithelial-mesenchymal transition of renal tubular epithelial cells by reducing reactive oxygen species production. Free Radic Res. 2012;46(2):174-83.

Yanagita M. Inhibitors/antagonists of TGF-β system in kidney fibrosis. Nephrol Dial Transplant. 2012;27(10): 3686-91.

Yang J, Liu Y. Dissection of key events in tubular epithelial to myofibroblast transition and its implications in renal interstitial fibrosis. Am J Pathol. 2001;159(4):1465-75.

Received for publication on 26th September 2018
Accepted for publication on 2th January 2019